Classifying BBHs from Pop. III stars with ET

Filippo Santoliquido

Ulyana Dupletsa, Jacopo Tissino, Marica Branchesi, Francesco Iacovelli,
Giuliano Iorio, Michela Mapelli, Davide Gerosa, Jan Harms, Mario Pasquato
worked on this

XIV ET symposium — Maastricht — May 6-10, 2024

GRAN SASSO SCIENCE INSTITUTE
SCHOOL OF ADVANCED STUDIES
Scuola Universitaria Superiore

INFN

VIRGO

EINSTEIN TELESCOPE

motivation

- Einstein Telescope will detect BBH mergers up to $z \sim 100$
- **high-redshift sources** with **low-SNR** and poor estimate of d_{L}
- **inferring the origin** of individual GW detections will not be granted

Ref. ***Maggiore et al. 2020***, ***Ng et al. 2021***, ***2022***, ***Branchesi et al. 2023***, ***Mancarella et al. 2023***

high-redshift sources

Pop. III stars:
peak of star formation at $z \sim 8 - 20$

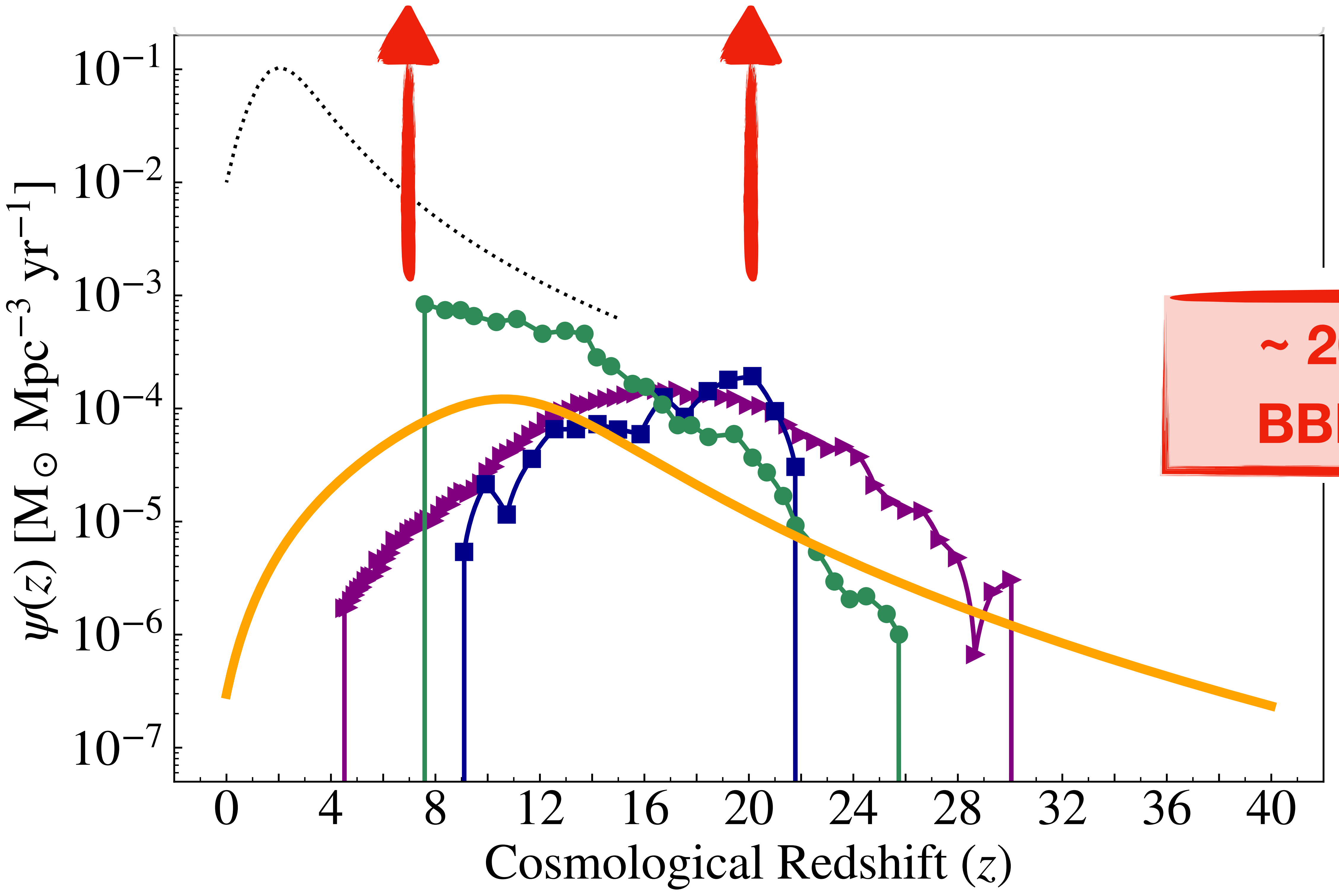

~ 20% - 70% of Pop. III BBHs mergers at $z \geq 8$

Ref. ***Santoliquido et al. 2023***

goal: classification

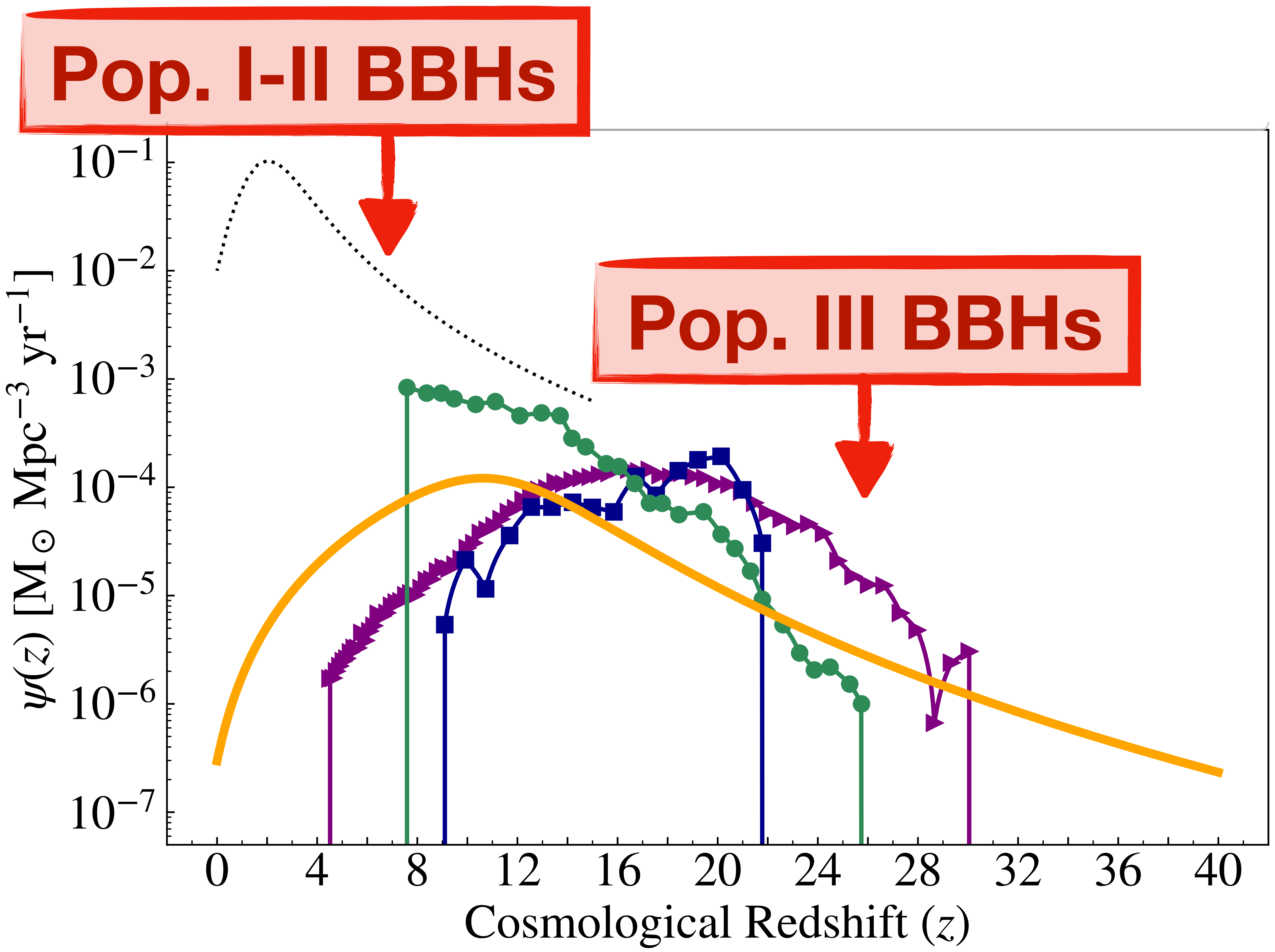

Ref. ***Santoliquido et al. 2023***, ***Santoliquido et al. 2024***

simulation-based classification

- A set of simulations presented in *Costa et al. 2023* and *Santoliquido et al. 2023*
- large parameter space to study mass and z evolution of Pop. III BBHs

Ref. ***Santoliquido et al. 2020*, *Iorio et al. 2023***

simulation-based classification

- A set of simulations presented in *Costa et al. 2023* and *Santoliquido et al. 2023*
- large parameter space to study mass and z evolution of Pop. III BBHs

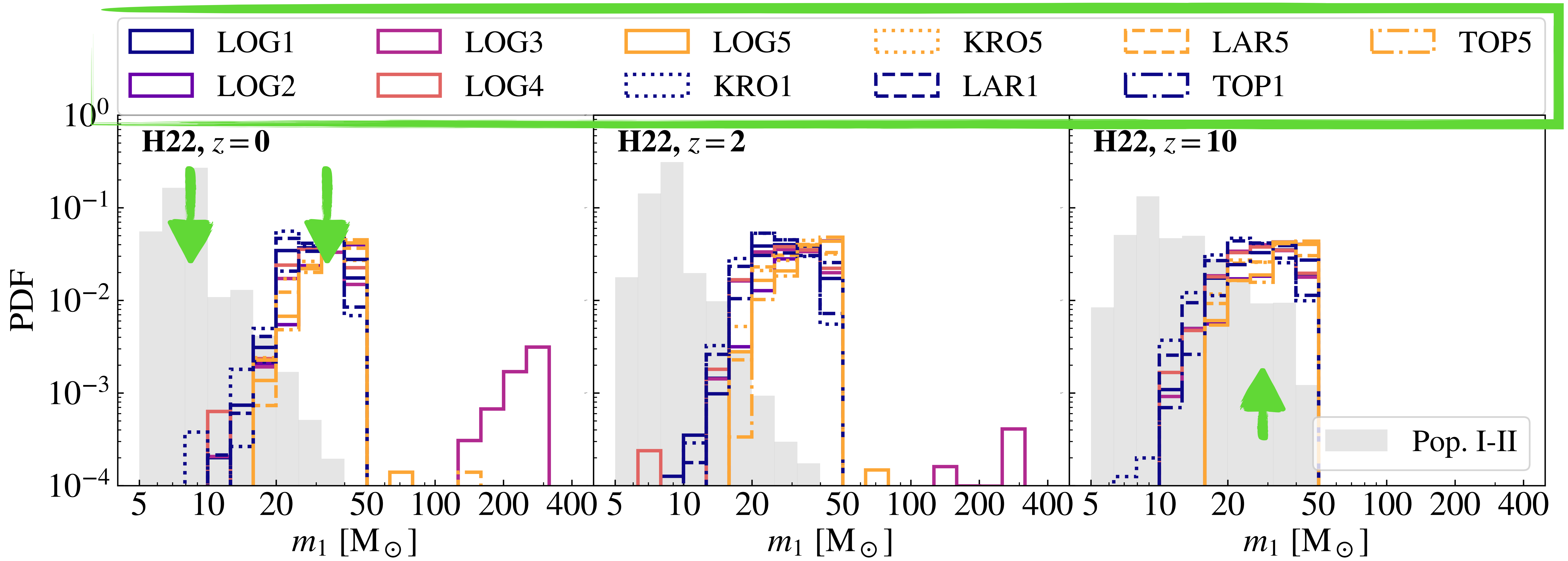

Ref. *Santoliquido et al. 2020*, *Iorio et al. 2023*

simulation-based classification

- A set of simulations presented in [Costa et al. 2023]() and [Santoliquido et al. 2023]()
- large parameter space to study mass and z evolution of Pop. III BBHs

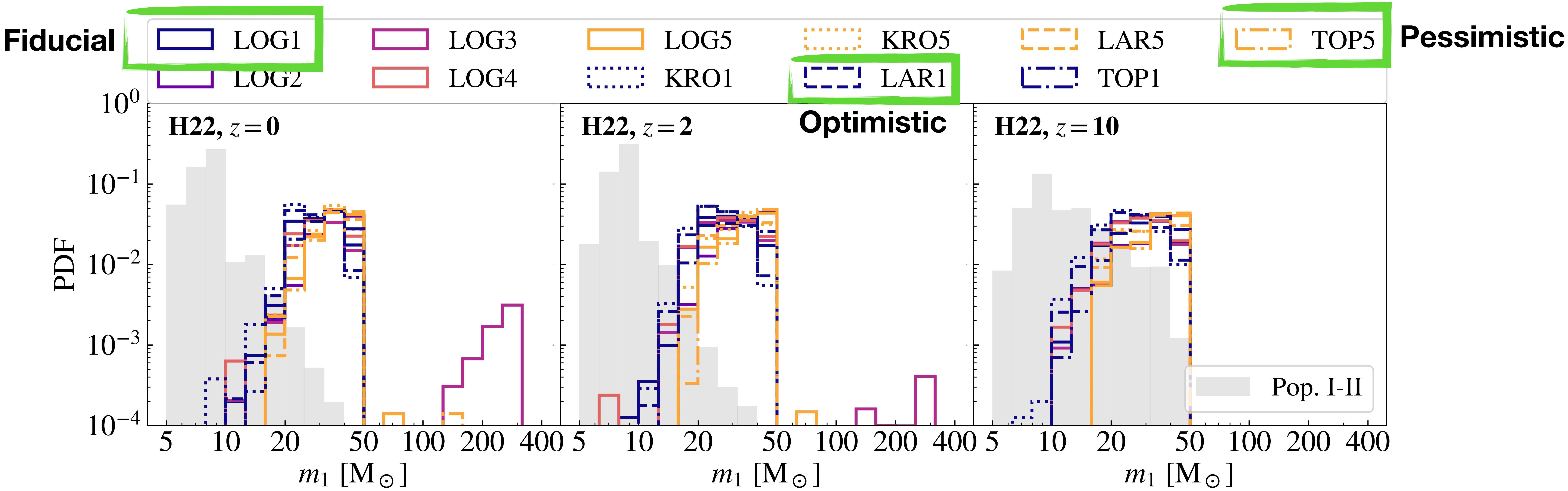

Ref. [Santoliquido et al. 2020](), [Iorio et al. 2023]()

how do we classify?

$$p(j \in k \,|\, d_i, \{\beta\}) = \int p(j \in k \,|\, x, d_j, \{\beta\}) \; p(x \,|\, d_j, \{\beta\})$$

Ref. ***Santoliquido et al. 2024***

how do we classify?

$$\boxed{p(j \in k \,|\, d_i, \{\beta\})} = \int p(j \in k \,|\, x, d_j, \{\beta\})\; p(x \,|\, d_j, \{\beta\})$$

this is the probability that the event j is a Pop. III BBH

Ref. ***Santoliquido et al. 2024***

how do we classify?

$$p(j \in k \,|\, d_i, \boxed{\{\beta\}}) = \int p(j \in k \,|\, x, d_j, \{\beta\})\; p(x \,|\, d_j, \{\beta\})$$

Fiducial $\beta_{III} \propto N_{\text{Pop. III}} \sim 400$

$\beta_{I-II} \propto N_{\text{Pop. I–II}} \sim 10^4$

Ref. *Santoliquido et al. 2024*

how do we classify?

$$p(j \in k \,|\, d_i, \{\beta\}) = \int p(j \in k \,|\, x, d_j, \{\beta\}) \boxed{p(x \,|\, d_j, \{\beta\})}$$

this is the posterior probability of waveform parameters

parameter-estimation performance of ET

Ref. ***[Santoliquido et al. 2024](), [Dupletsa et al. 2023]()***

how do we classify?

$$p(j \in k \mid d_i, \{\beta\}) = \int p(j \in k \mid x, d_j, \{\beta\}) \, \boxed{p(x \mid d_j, \{\beta\})}$$

this is the posterior probability of waveform parameters

GWFISH

Ulyana Dupletsa's talk later today

Ref. *Santoliquido et al. 2024*, *Dupletsa et al. 2023*

how do we classify?

$$p(j \in k \mid d_i, \{\beta\}) = \int \boxed{p(j \in k \mid x, d_j, \{\beta\})}\, p(x \mid d_j, \{\beta\})$$

this is the probability that links waveform parameters to Pop. III BBHs

Ref. *Santoliquido et al. 2024*, *Ng et al. 2022*, *Berbel et al. 2023*

how do we classify?

$$p(j \in k \,|\, d_i, \{\beta\}) = \int \boxed{p(j \in k \,|\, x, d_j, \{\beta\})}\; p(x \,|\, d_j, \{\beta\})$$

easiest approach is to consider a fix threshold

Ref. *Santoliquido et al. 2024*, *Ng et al. 2022*, *Berbel et al. 2023*

$$p(j \in k \,|\, d_i, \{\beta\}) = \int \boxed{p(j \in k \,|\, x, d_j, \{\beta\})}\; p(x \,|\, d_j, \{\beta\})$$

$$= 1 \quad \text{if} \quad m_{1,\mathrm{d}} \gtrsim 60\ \mathrm{M}_\odot$$

Ref. *Santoliquido et al. 2024*

$$\boxed{p(j \in k \,|\, d_i, \{\beta\})} = \int \boxed{p(j \in k \,|\, x, d_j, \{\beta\})}\, p(x \,|\, d_j, \{\beta\})$$

$= 1 \quad \text{if} \quad m_{1,\mathrm{d}} \gtrsim 60\ \mathrm{M}_\odot$

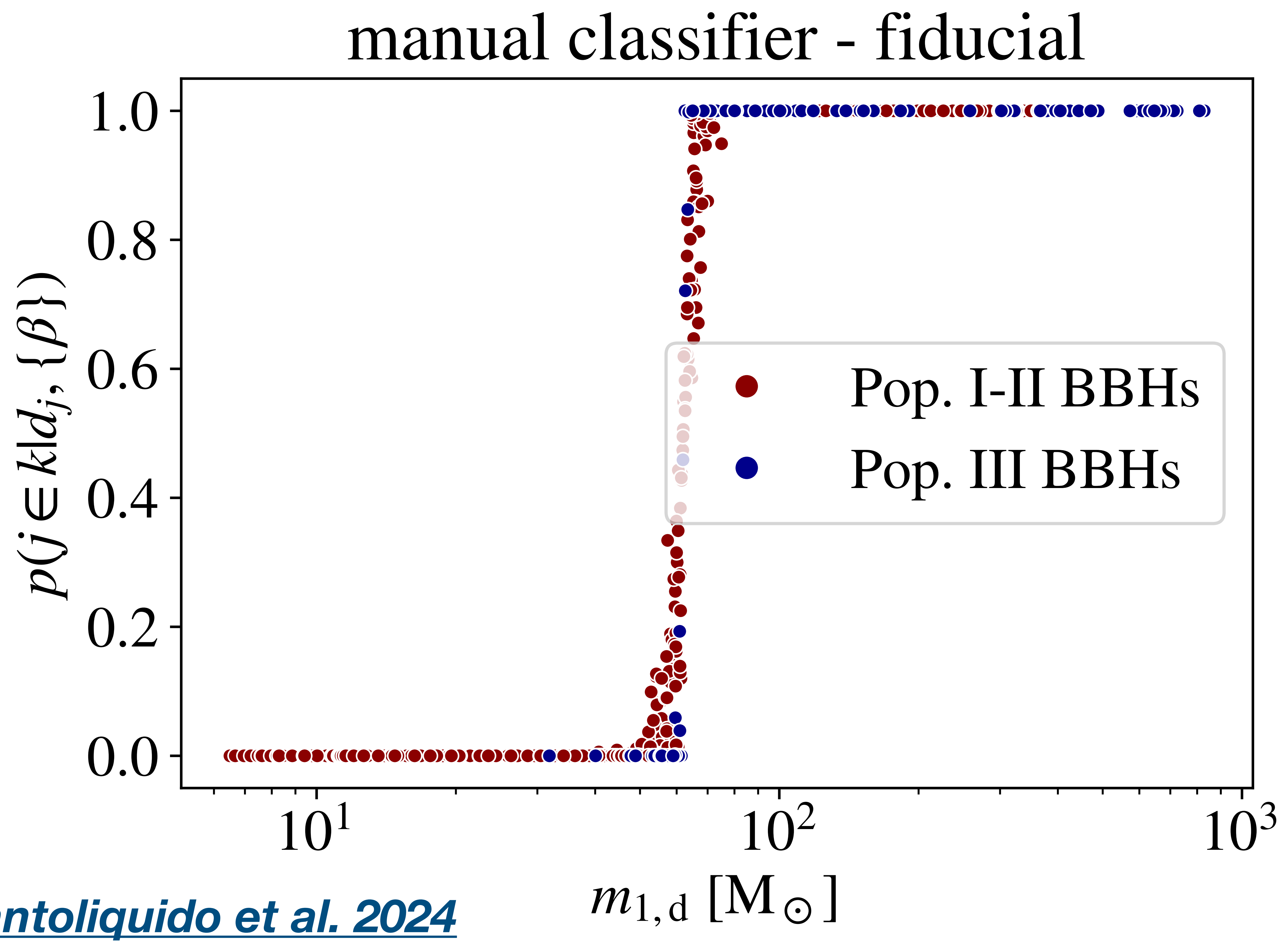

⚠️ precision is ~ 0.16

Ref. *Santoliquido et al. 2024*

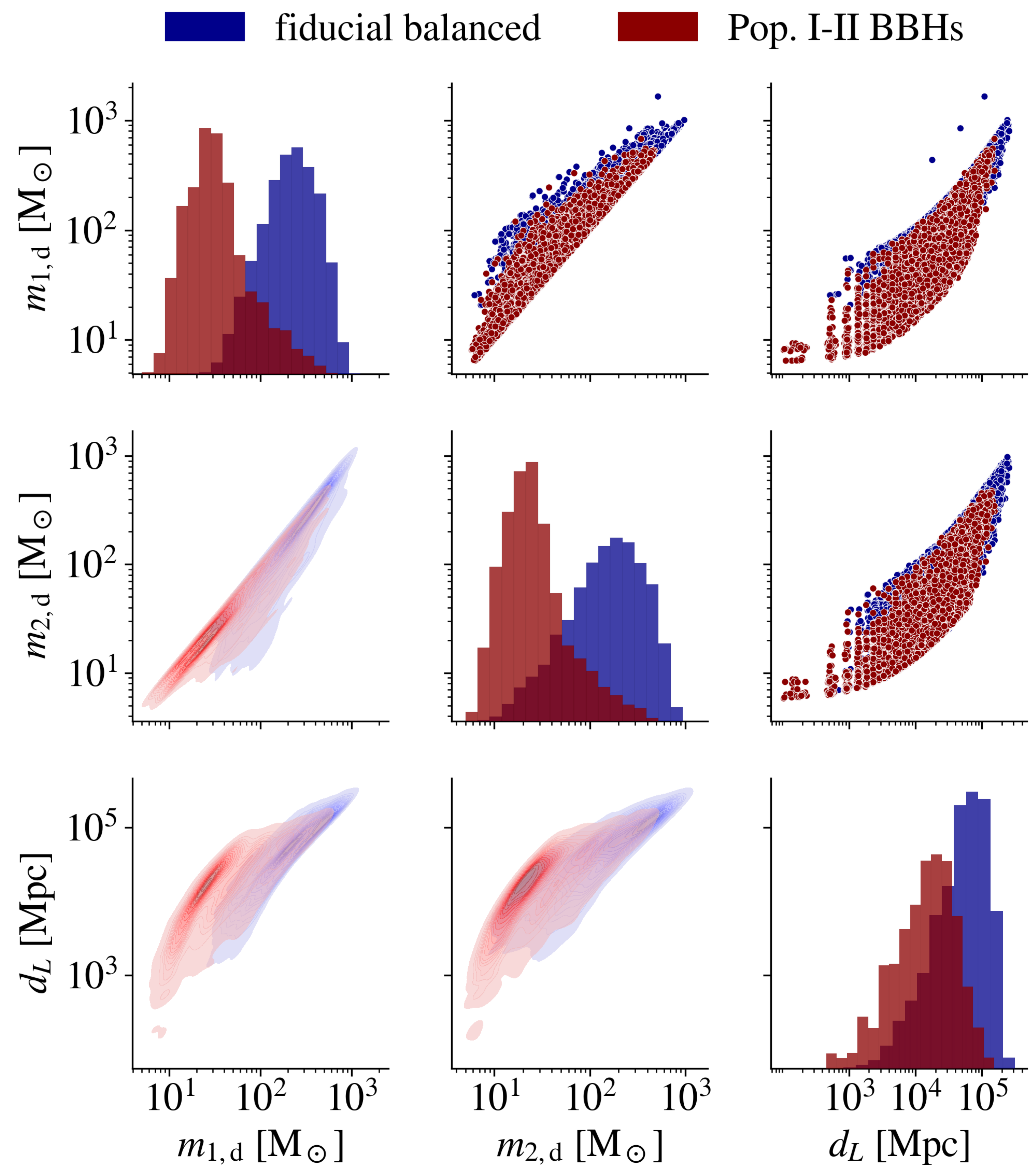

Ref. [*Santoliquido et al. 2024*]

Pop. I-II BBHs and Pop. III BBHs do **overlap**

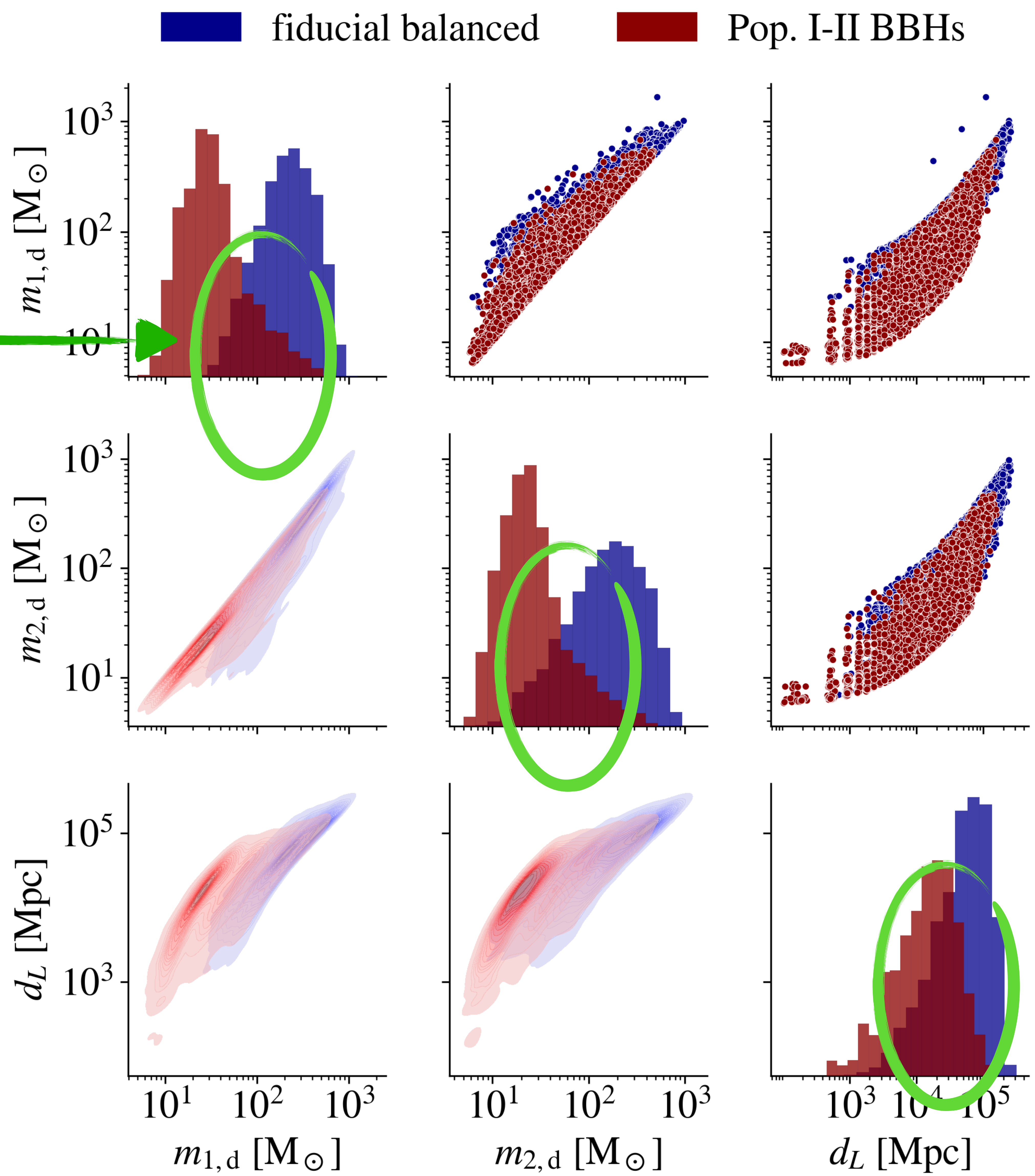

Ref. [*Santoliquido et al. 2024*]

$$p(j \in k \,|\, d_i, \{\beta\}) = \int \boxed{p(j \in k \,|\, x, d_j, \{\beta\})} \; p(x \,|\, d_j, \{\beta\})$$

we can use Machine Learning XGBoost

supervised learning based on decision trees

Ref. *Santoliquido et al. 2024*, *Chen et al. 2016*, *Pedregosa et al. 2012*, *Antonelli et. al 2023*

$$p(j \in k \,|\, d_i, \{\beta\}) = \int \boxed{p(j \in k \,|\, x, d_j, \{\beta\})}\, p(x \,|\, d_j, \{\beta\})$$

we can use Machine Learning

XGBoost

FP>FN

precision = TP/(TP+FP)

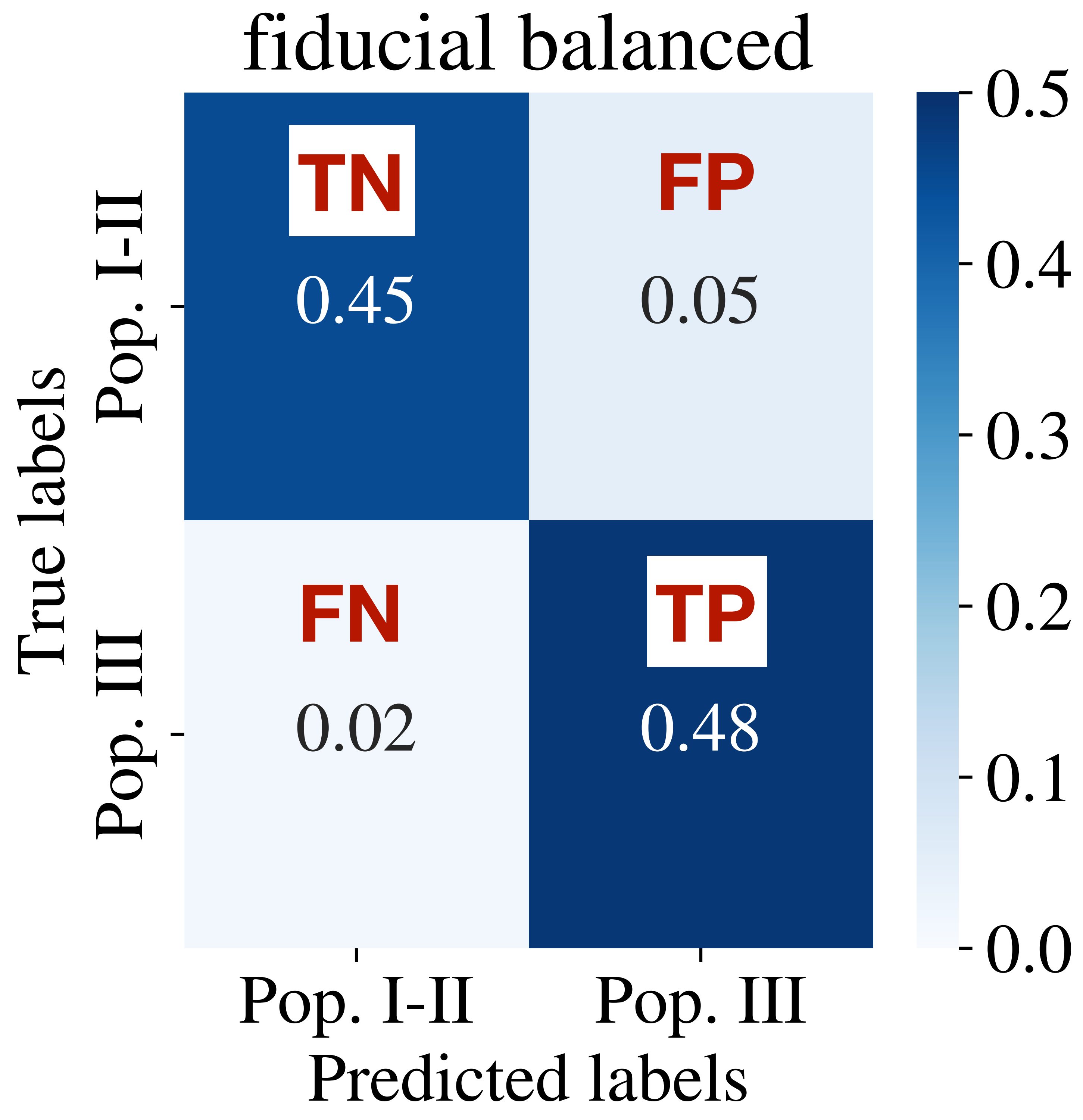

Ref. ***Santoliquido et al. 2024***

$$p(j \in k \,|\, d_i, \{\beta\}) = \int \boxed{p(j \in k \,|\, x, d_j, \{\beta\})}\; p(x \,|\, d_j, \{\beta\})$$

we can use Machine Learning

XGBoost

high precision > 0.90

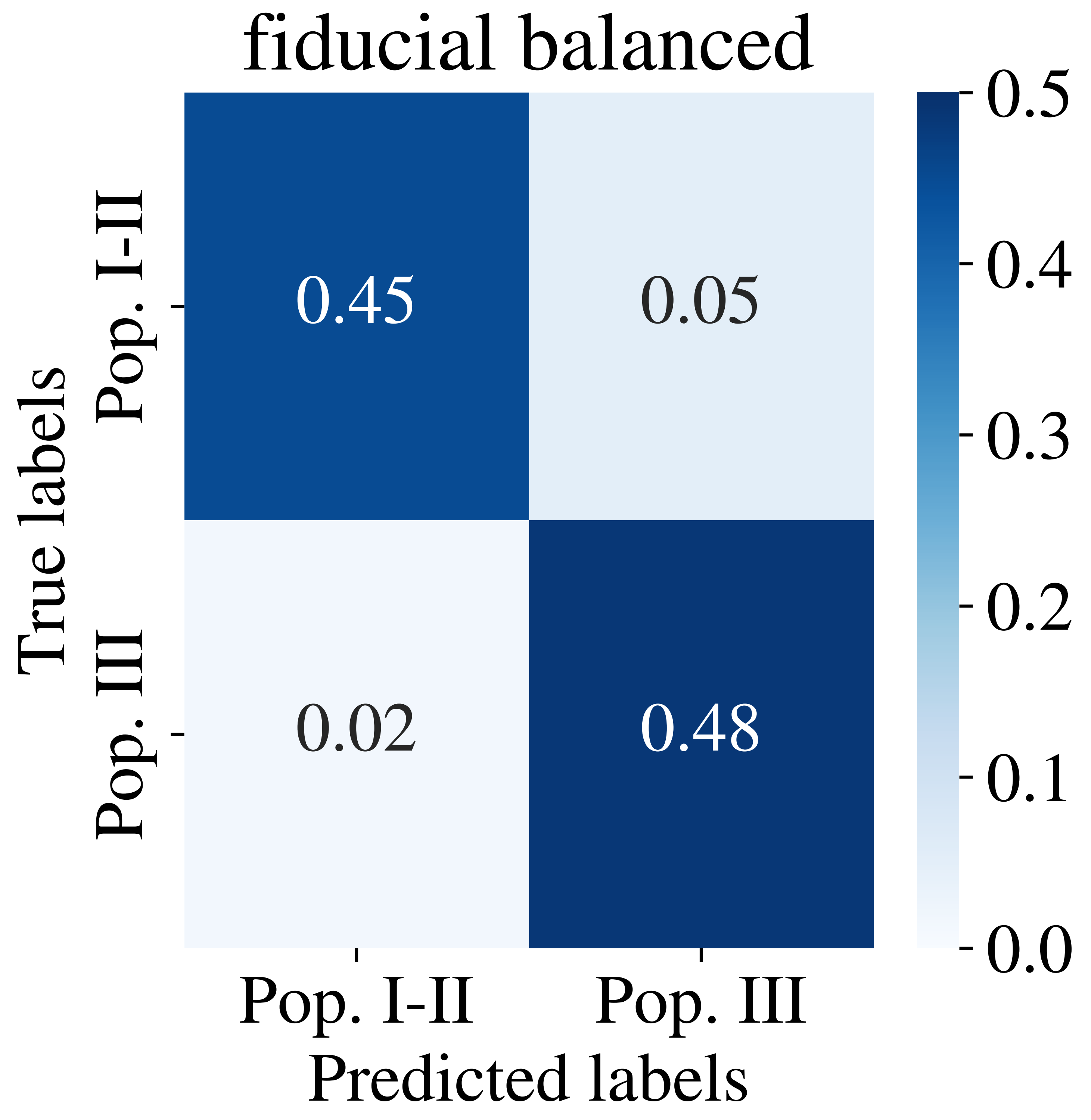

* trained and tested on balanced classes

* instances: > 10^4

Ref. [*Santoliquido et al. 2024*]

$$\boxed{p(j \in k \,|\, d_i, \{\beta\})} = \int \boxed{p(j \in k \,|\, x, d_j, \{\beta\})}\, p(x \,|\, d_j, \{\beta\})$$

we can use Machine Learning

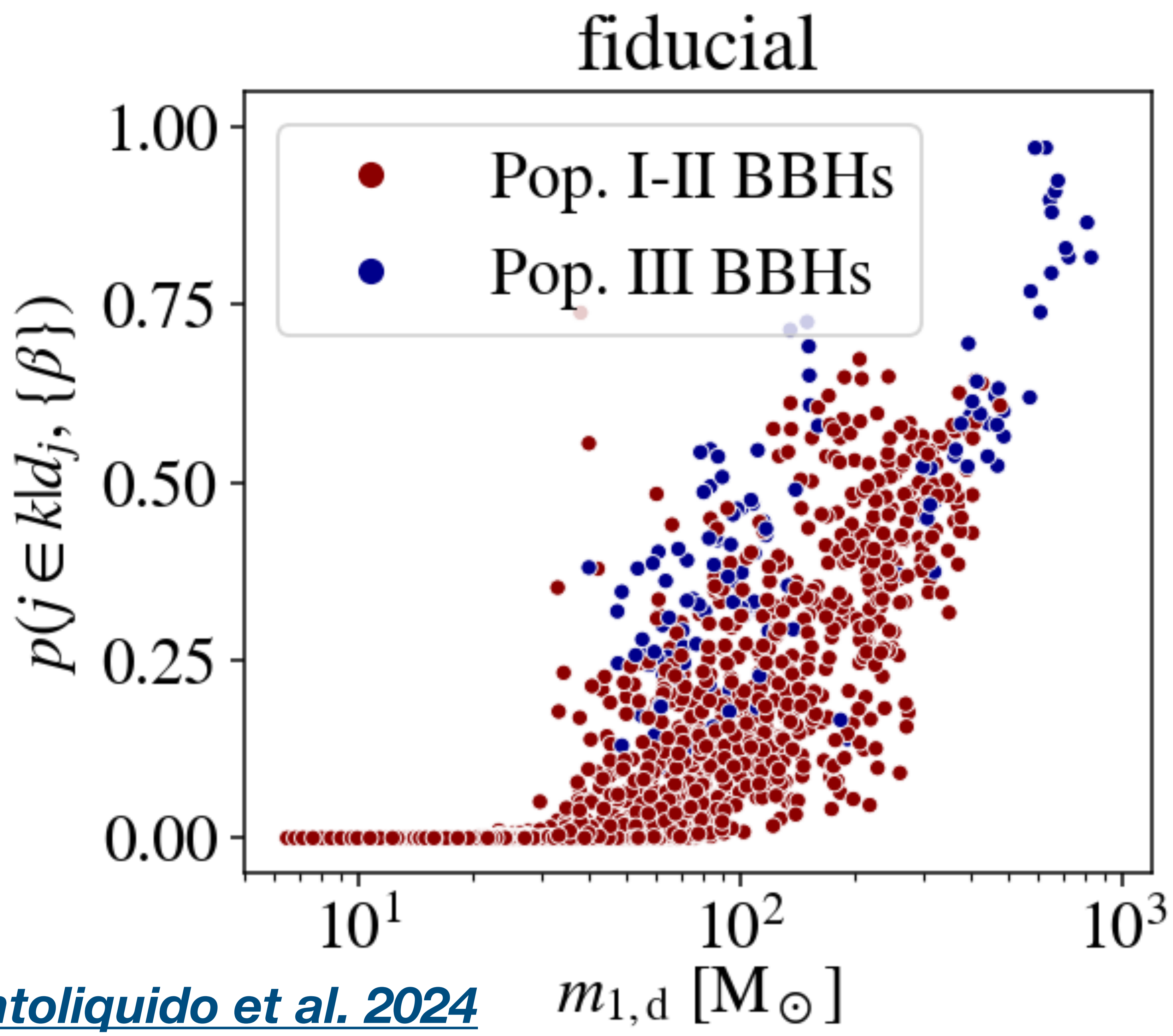

~10% of detected sources are classified with precision > 0.90

Ref. ***Santoliquido et al. 2024***

$$\boxed{p(j \in k \,|\, d_i, \{\beta\})} = \int \boxed{p(j \in k \,|\, x, d_j, \{\beta\})}\; p(x \,|\, d_j, \{\beta\})$$

we can use Machine Learning

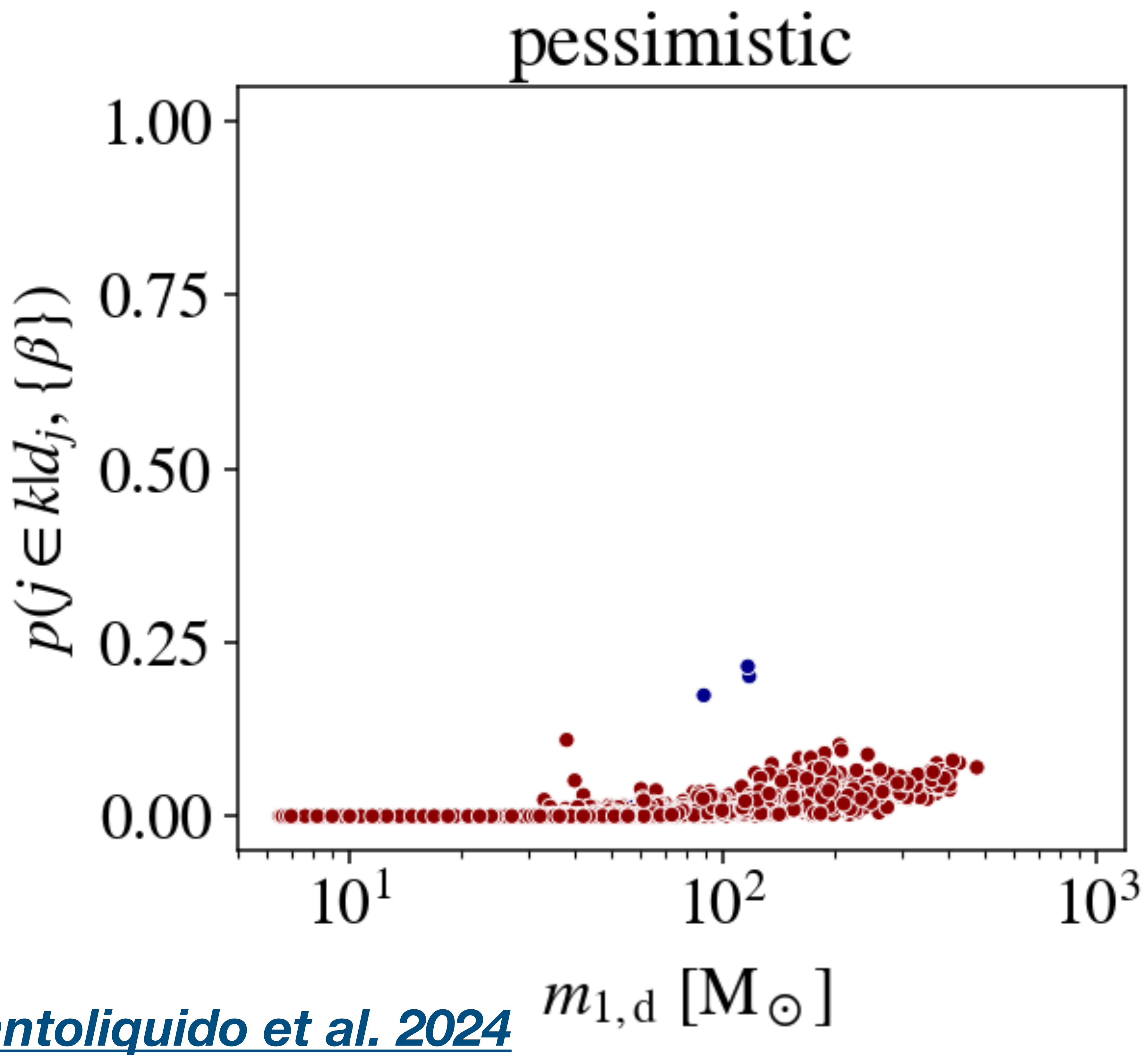

~30% of detected sources are classified with precision > 0.90

Ref. ***Santoliquido et al. 2024***

$$\boxed{p(j \in k \,|\, d_i, \{\beta\})} = \int \boxed{p(j \in k \,|\, x, d_j, \{\beta\})}\; p(x \,|\, d_j, \{\beta\})$$

we can use Machine Learning

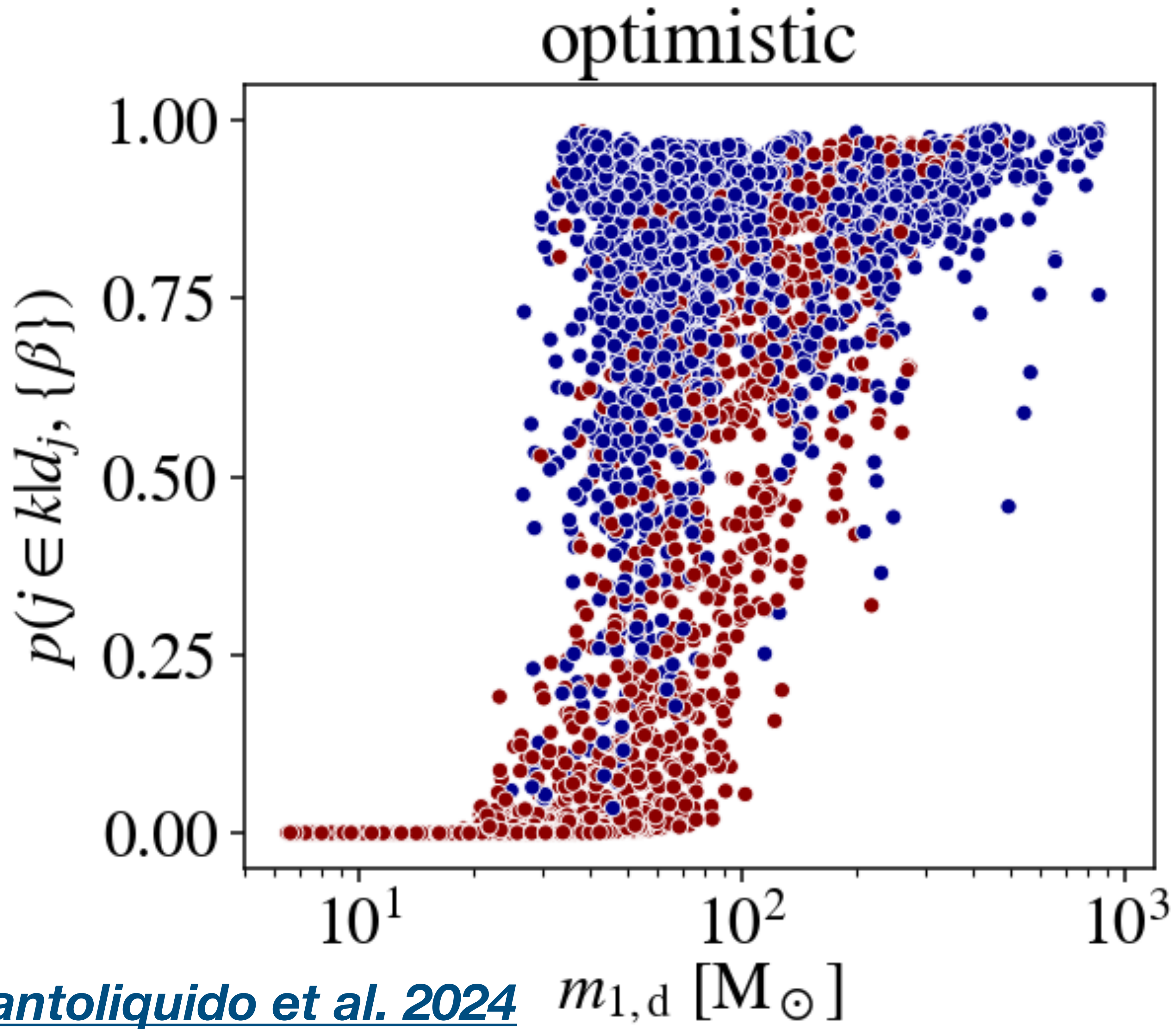

~45% of detected sources are classified with precision > 0.90

Ref. ***Santoliquido et al. 2024***

conclusions

- machine learning boosts our ability to classify high-redshift sources
- A subset of sources (~10 %) can be classified with high precision (~0.90)
- This methodology can be easily extended to include other formation channels

Ref. ***Santoliquido et al. 2024***

Backup slides

Intro

Population-synthesis

αλ formalism for modelling the common envelope

- $\Delta E = \alpha(E_{\rm b,f} - E_{\rm b,i}) = \alpha \frac{G m_{\rm c1} m_{\rm c2}}{2} \left(\frac{1}{a_{\rm f}} - \frac{1}{a_{\rm i}} \right)$ This is the orbital energy before and after the common envelope phase
- $E_{\rm env} = \frac{G}{\lambda} \left[\frac{m_{\rm env,1} m_1}{R_1} + \frac{m_{\rm env,2} m_2}{R_2} \right]$ This is the binding energy of the envelope
- By imposing $\Delta E = E_{\rm env}$, $\frac{1}{a_{\rm f}} = \frac{1}{\alpha\lambda} \frac{2}{m_{\rm c1} m_{\rm c2}} \left[\frac{m_{\rm env,1} m_1}{R_1} + \frac{m_{\rm env,2} m_2}{R_2} \right] + \frac{1}{a_i}$
- If α is larger, $a_{\rm f}$ is larger, following $a_{\rm f} \sim \frac{\alpha}{1+\alpha}$. Therefore larger α gets wider binaries
- Where λ is the parameter which measures the concentration of the envelope (the smaller λ is, the more concentrated is the envelope).
- The $\alpha\lambda$ formalism is a simplified prescription. When $\alpha > 1$, we account for other sources of energy that make the envelope less bind, for instance recombination energy. Recent works (e.g. *Fragos et al. 2019*) suggest that $\alpha > 1$ is necessary to reproduce the final orbital separation obtained with hydrodynamical simulations.

$$\mathcal{R}(z) = \int_{z_{\max}}^{z} \left[\int_{Z_{\min}}^{Z_{\max}} \boxed{\mathrm{SFRD}(z', Z)} \boxed{\mathcal{F}(z', z, Z)} \mathrm{d}Z \right] \frac{\mathrm{d}t(z')}{\mathrm{d}z'} \mathrm{d}z'$$

Santoliquido et al. 2020:
https://arxiv.org/pdf/2004.09533.pdf

COSMORATE

Santoliquido et al. 2020:
https://arxiv.org/pdf/2004.09533.pdf

$$\mathcal{R}(z) = \int_{z_{\max}}^{z} \left[\int_{Z_{\min}}^{Z_{\max}} \boxed{\mathrm{SFRD}(z', Z)} \boxed{\mathcal{F}(z', z, Z)} \mathrm{d}Z \right] \frac{\mathrm{d}t(z')}{\mathrm{d}z'} \mathrm{d}z'$$

Evaluated from our population-synthesis catalogs:

$$\mathcal{F}(z', z, Z) = \frac{1}{\mathcal{M}_{\mathrm{TOT}}(Z)} \frac{\mathrm{d}\mathcal{N}(z', z, Z)}{\mathrm{d}t(z)}$$

COSMORATE

$$\mathcal{R}(z) = \int_{z_{\max}}^{z} \left[\int_{Z_{\min}}^{Z_{\max}} \boxed{\mathrm{SFRD}(z', Z)} \boxed{\mathcal{F}(z', z, Z)} \mathrm{d}Z \right] \frac{\mathrm{d}t(z')}{\mathrm{d}z'} \mathrm{d}z'$$

Santoliquido et al. 2020:
https://arxiv.org/pdf/2004.09533.pdf

$$\mathrm{SFRD}(z, Z) = \boxed{\psi(z)} \boxed{p(Z|z)}$$

Evaluated from our population-synthesis catalogs:

$$\mathcal{F}(z', z, Z) = \frac{1}{\mathcal{M}_{\mathrm{TOT}}(Z)} \frac{\mathrm{d}\mathcal{N}(z', z, Z)}{\mathrm{d}t(z)}$$

COSMORATE

$$\mathcal{R}(z) = \int_{z_{\max}}^{z} \left[\int_{Z_{\min}}^{Z_{\max}} \boxed{\mathrm{SFRD}(z', Z)}\,\boxed{\mathcal{F}(z', z, Z)}\,\mathrm{d}Z\right] \frac{\mathrm{d}t(z')}{\mathrm{d}z'}\mathrm{d}z'$$

Santoliquido et al. 2020:
https://arxiv.org/pdf/2004.09533.pdf

$$\mathrm{SFRD}(z, Z) = \boxed{\psi(z)}\,\boxed{p(Z|z)}$$

Evaluated from our population-synthesis catalogs:

$$\mathcal{F}(z', z, Z) = \frac{1}{\mathcal{M}_{\mathrm{TOT}}(Z)} \frac{\mathrm{d}\mathcal{N}(z', z, Z)}{\mathrm{d}t(z)}$$

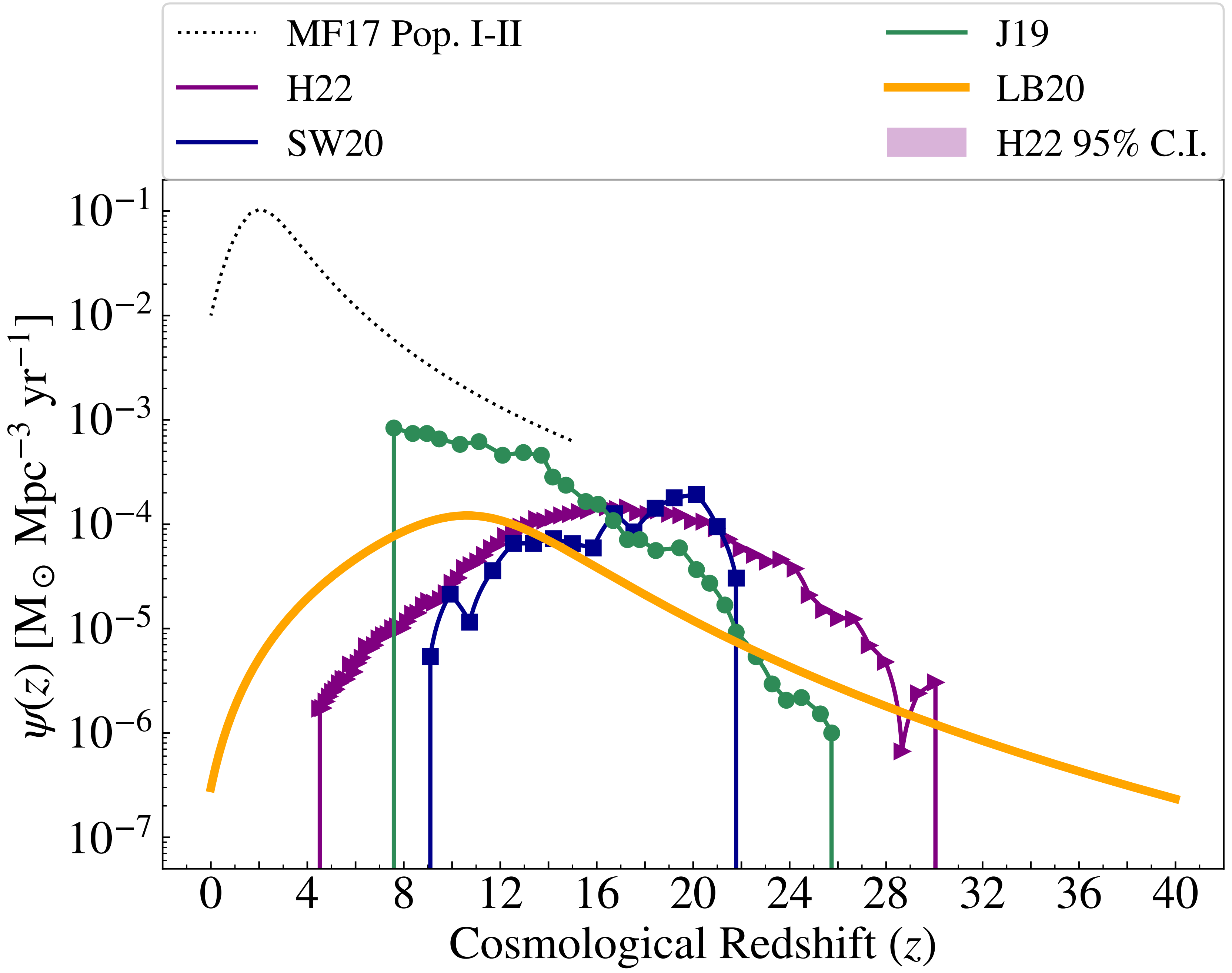

We considered four different estimates of Pop. III SFRD:

H22 - *Hartwig et al. 2022*
J19 - *Jaacks et al. 2019*
LB20 - *Liu & Bromm 2020*
SW20 - *Skinner & Wise 2020*

Santoliquido et al. 2023:
https://arxiv.org/pdf/2303.15515.pdf

Paper 4

Initial conditions

Costa et al. 2023

Table 1. Initial conditions.

Model	$M_{ZAMS,1}$	M_{ZAMS}	q	P	e
LOG1	Flat in log	–	S12	S12	S12
LOG2	Flat in log	–	S12	SB13	Thermal
LOG3	–	Flat in log	Sorted	S12	S12
LOG4	Flat in log	–	SB13	S12	Thermal
LOG5	Flat in log	–	SB13	SB13	Thermal
KRO1	K01	–	S12	S12	S12
KRO5	K01	–	SB13	SB13	Thermal
LAR1	L98	–	S12	S12	S12
LAR5	L98	–	SB13	SB13	Thermal
TOP1	Top heavy	–	S12	S12	S12
TOP5	Top heavy	–	SB13	SB13	Thermal

Column 1 reports the model name. Column 2 describes how we generate the ZAMS mass of the primary star (i.e., the most massive of the two members of the binary system). Column 3 describes how we generate the ZAMS mass of the overall stellar population (without differentiating between primary and secondary stars). We follow this procedure only for model LOG3 (see the text for details). Columns 4, 5, and 6 specify the distributions we used to generate the mass ratios q, the orbital periods P and the orbital eccentricity e. See Section 2.2 for a detailed description of these distributions.

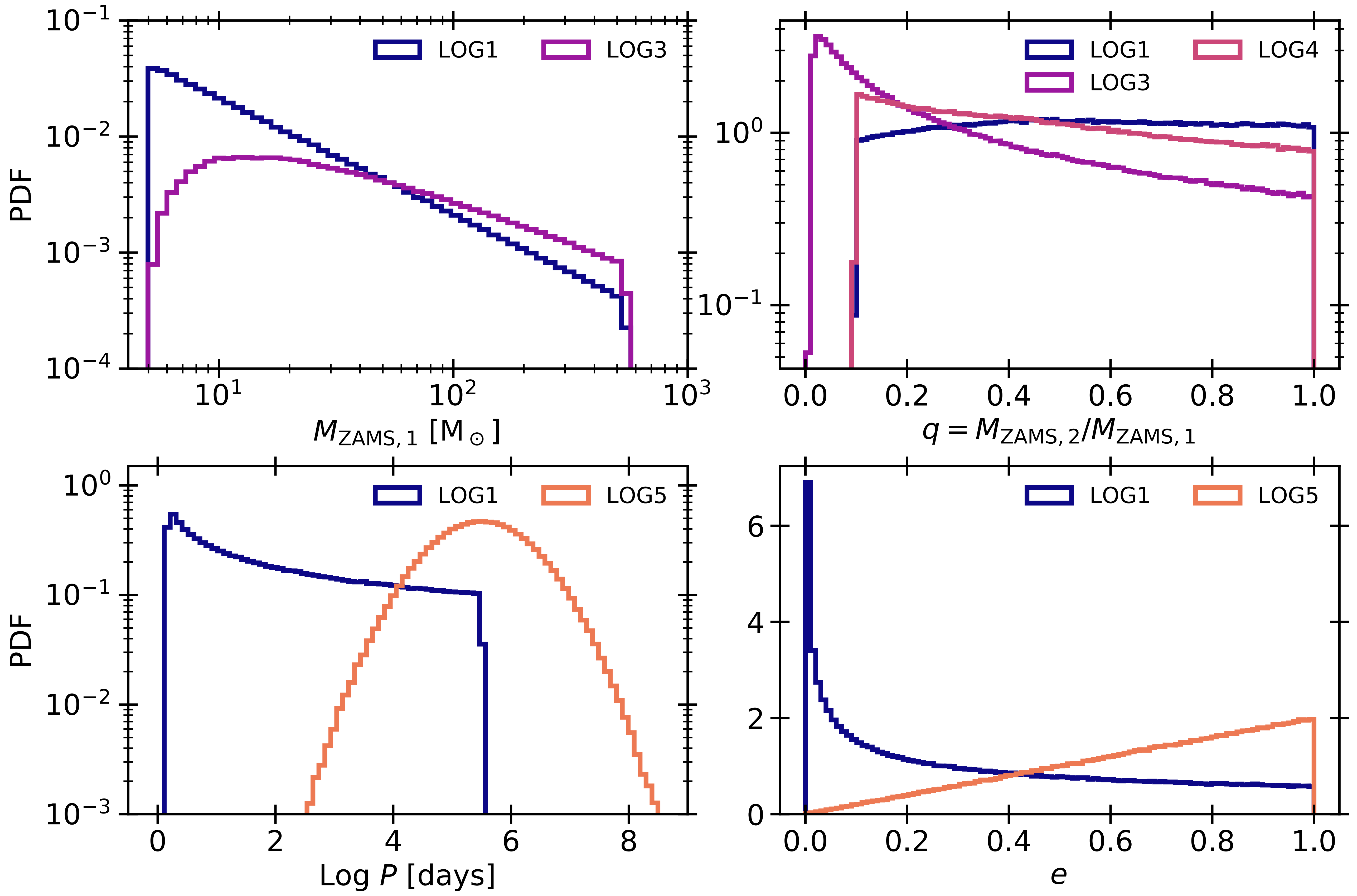

Figure 3. Initial conditions for the models LOG1–5. From upper left to bottom right: ZAMS mass of the primary star $M_{ZAMS,1}$, mass ratio $q = M_{ZAMS,2}/M_{ZAMS,1}$, initial orbital period P, and initial orbital eccentricity e. In the upper-left panel, we do not show models LOG2, LOG4 and LOG5 for simplicity, because they follow the same distribution as LOG1 (i.e., $M_{ZAMS,1}$ is sampled from a flat-in-log distribution), while in model LOG3 we sample the entire stellar population (i.e., both primary and secondary stars) from a flat-in-log distribution. In the upper-righ panel (q), model LOG2 follows the same distribution as LOG1 (S12), while model LOG5 follows the same distribution as LOG4 (SB13). In the lower-left panel (P), models LOG3 and LOG4 follow the same distribution as LOG1 (S12), while models LOG2 and LOG5 are sampled from SB13. Finally, in the lower-right panel (e), models LOG1 and LOG3 follow S12, while the other models adopt a thermal distribution (we show only LOG5 for simplicity). Table 1 describes the models in detail.

Santoliquido et al. 2023:
https://arxiv.org/pdf/2303.15515.pdf

Pop. III BBHs: mass evolution

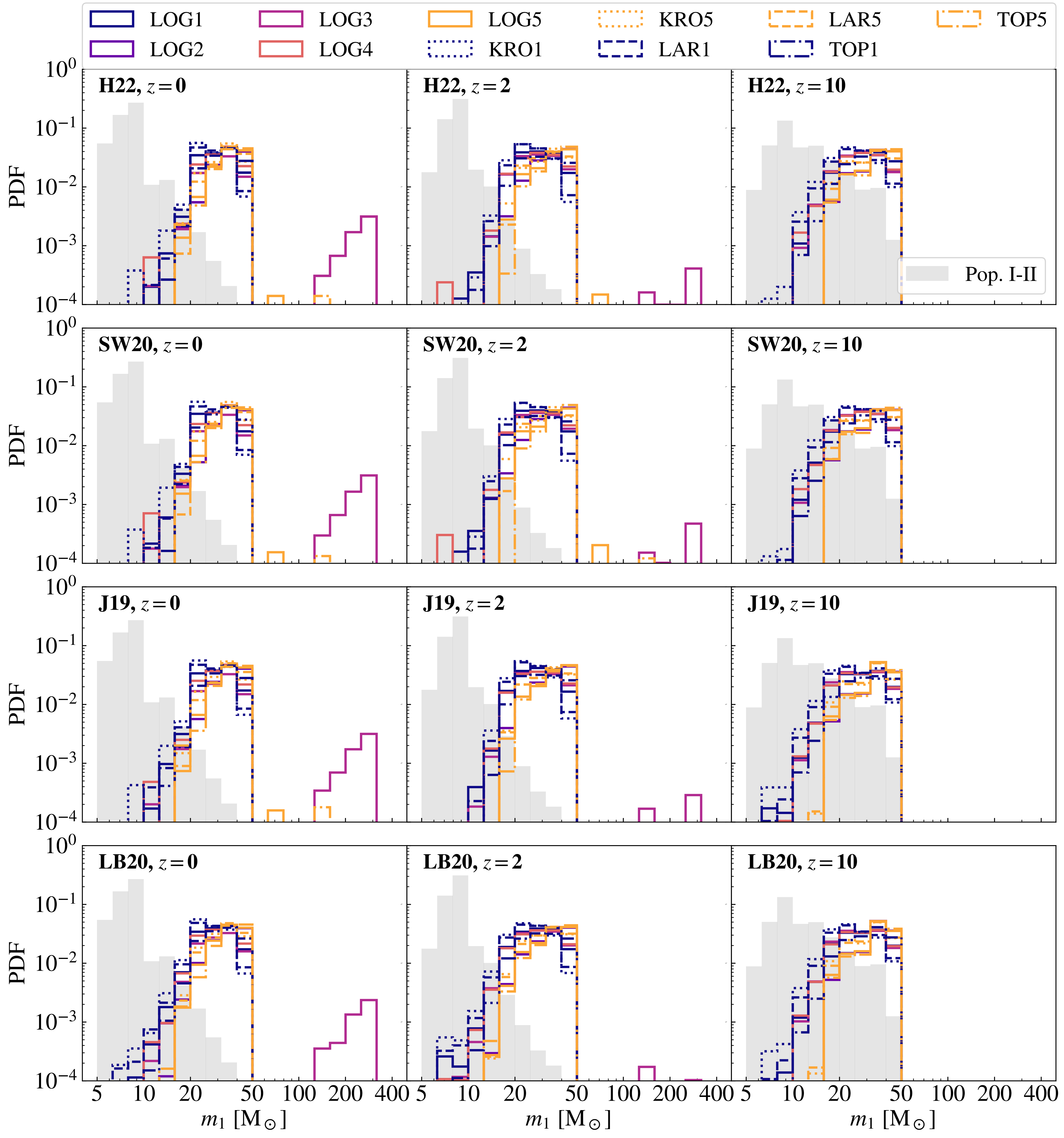

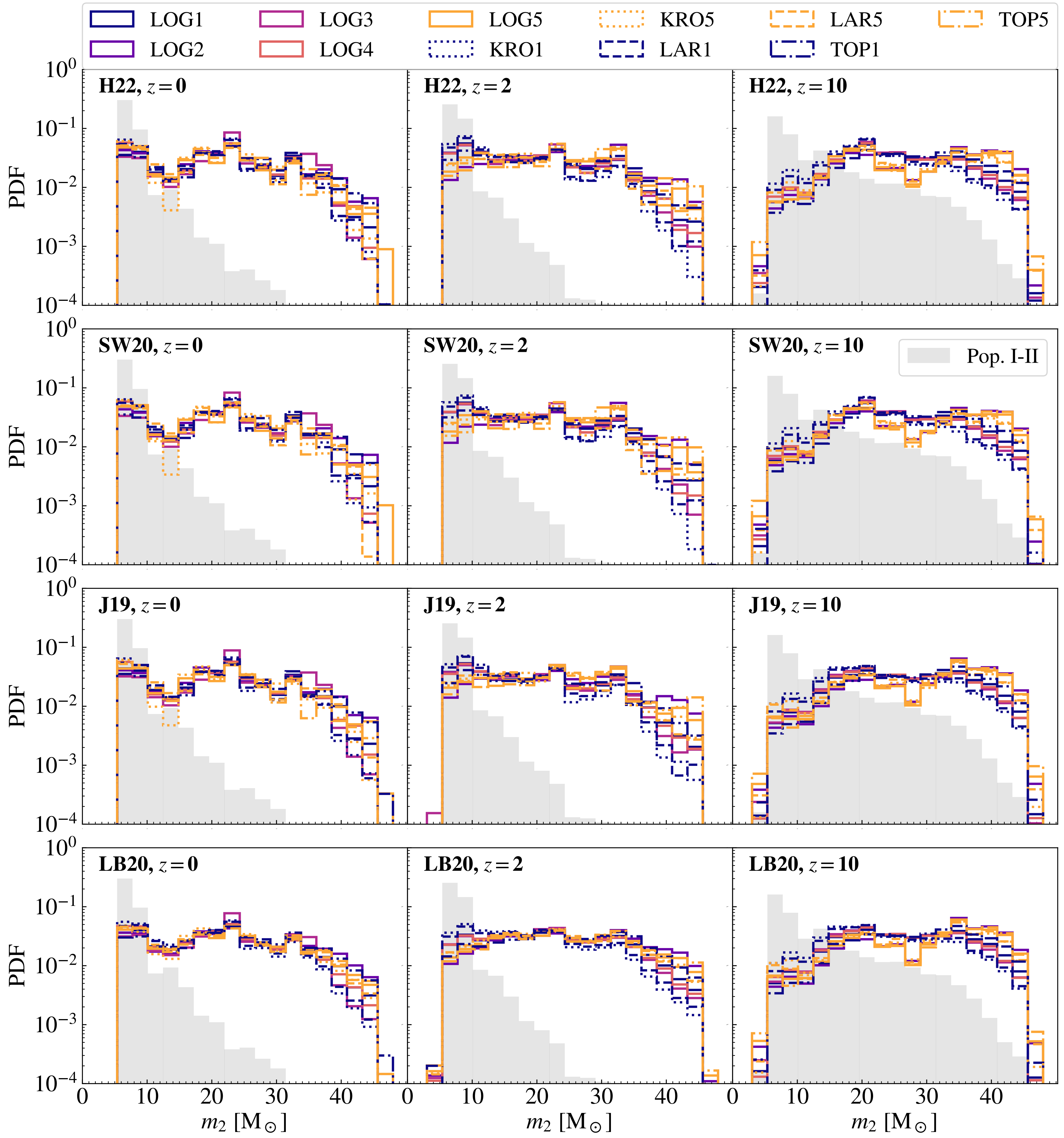

detection rate

$$\mathcal{R}_{\rm det} = \int \frac{\mathrm{d}^2\mathcal{R}(m_1, m_2, z)}{\mathrm{d}m_1 \mathrm{d}m_2} \frac{1}{(1+z)} \frac{\mathrm{d}V_c}{\mathrm{d}z}\, p_{\rm det}(m_1, m_2, z)\, \mathrm{d}m_1\, \mathrm{d}m_2\, \mathrm{d}z$$

$$\frac{\mathrm{d}^2\mathcal{R}(m_1, m_2, z)}{\mathrm{d}m_1 \mathrm{d}m_2} = \mathcal{R}(z)\, p(m_1, m_2|z)$$

$$\rho = \rho_{\rm opt} \sqrt{\omega_0^2 + \omega_1^2 + \omega_2^2}$$

$$\rho_{\rm opt}^2 = 4 \int_{f_{\rm low}}^{f_{\rm high}} \mathrm{d}f\, \frac{|\tilde{h}(f)|^2}{S_n(f)}$$

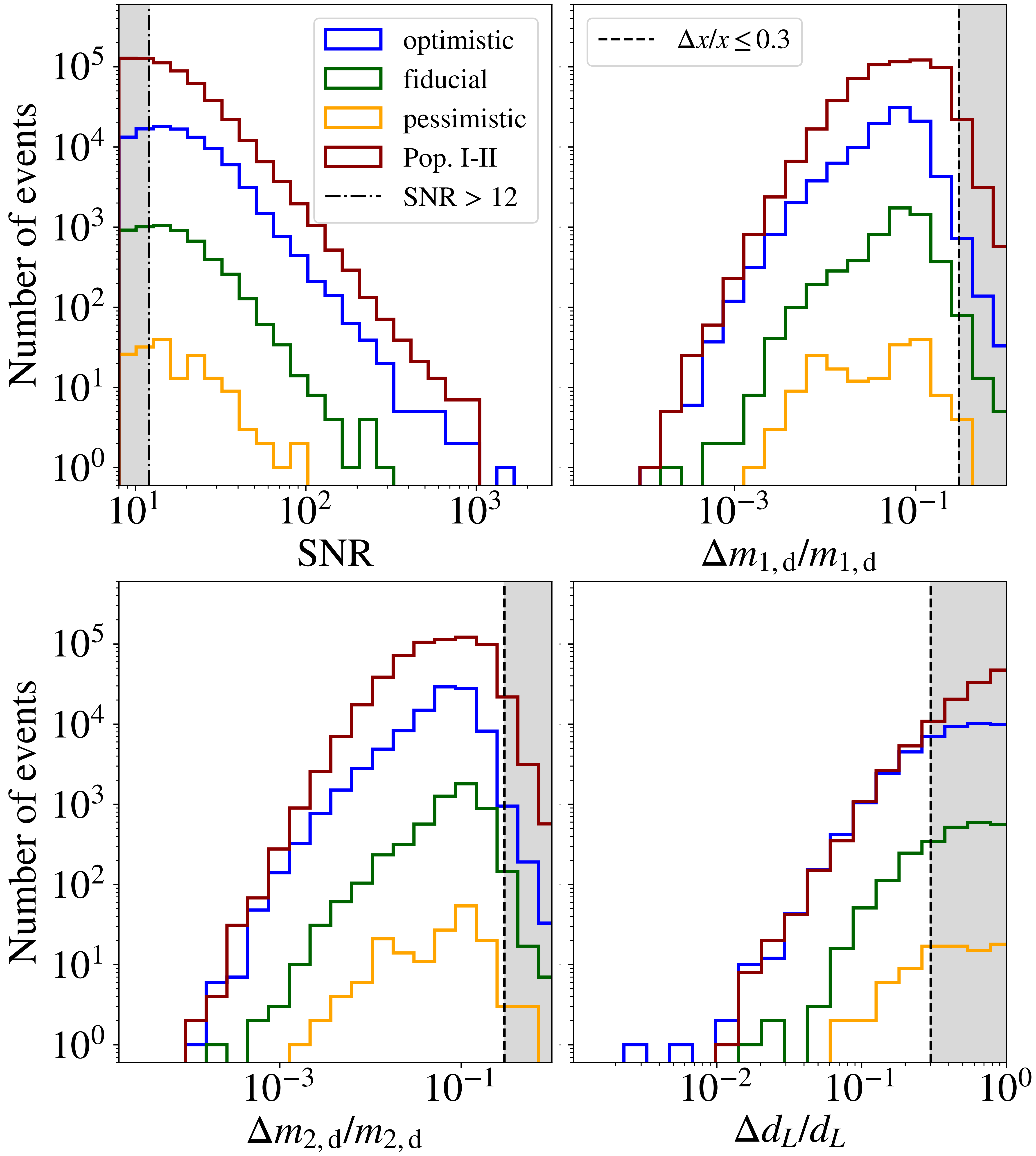
optimistic
fiducial
pessimistic
Pop. I-II
SNR > 12
Δx/x ≤ 0.3
Number of events
SNR
Δm_{1,d}/m_{1,d}
Δm_{2,d}/m_{2,d}
Δd_L/d_L

$$p(j \in k \,|\, x, d_j, \{\beta\}) = 1 \quad \text{if} \quad m_{1,\mathrm{d}} \gtrsim 60\ \mathrm{M}_\odot$$

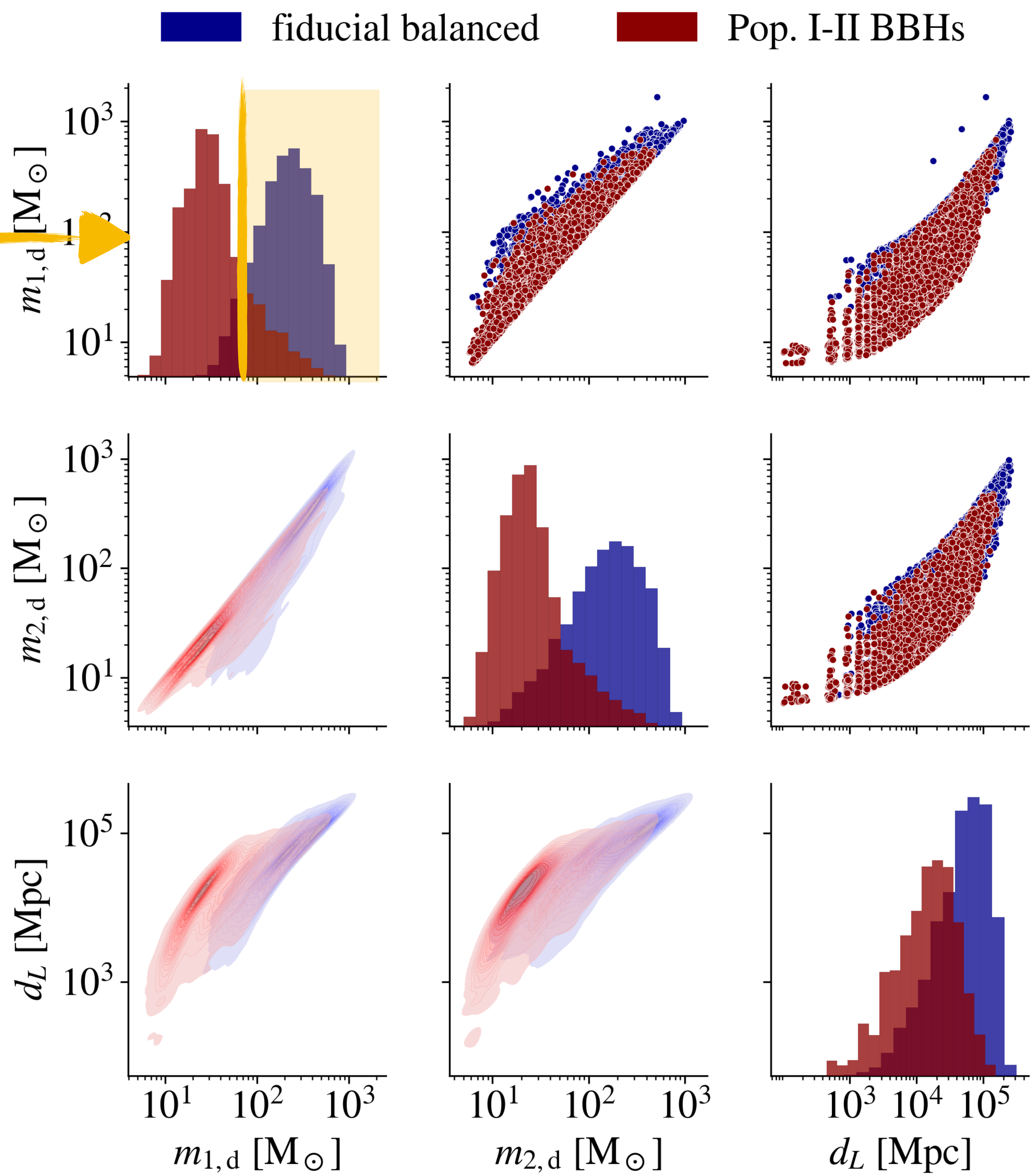

Ref. [*Santoliquido et al. 2024*]

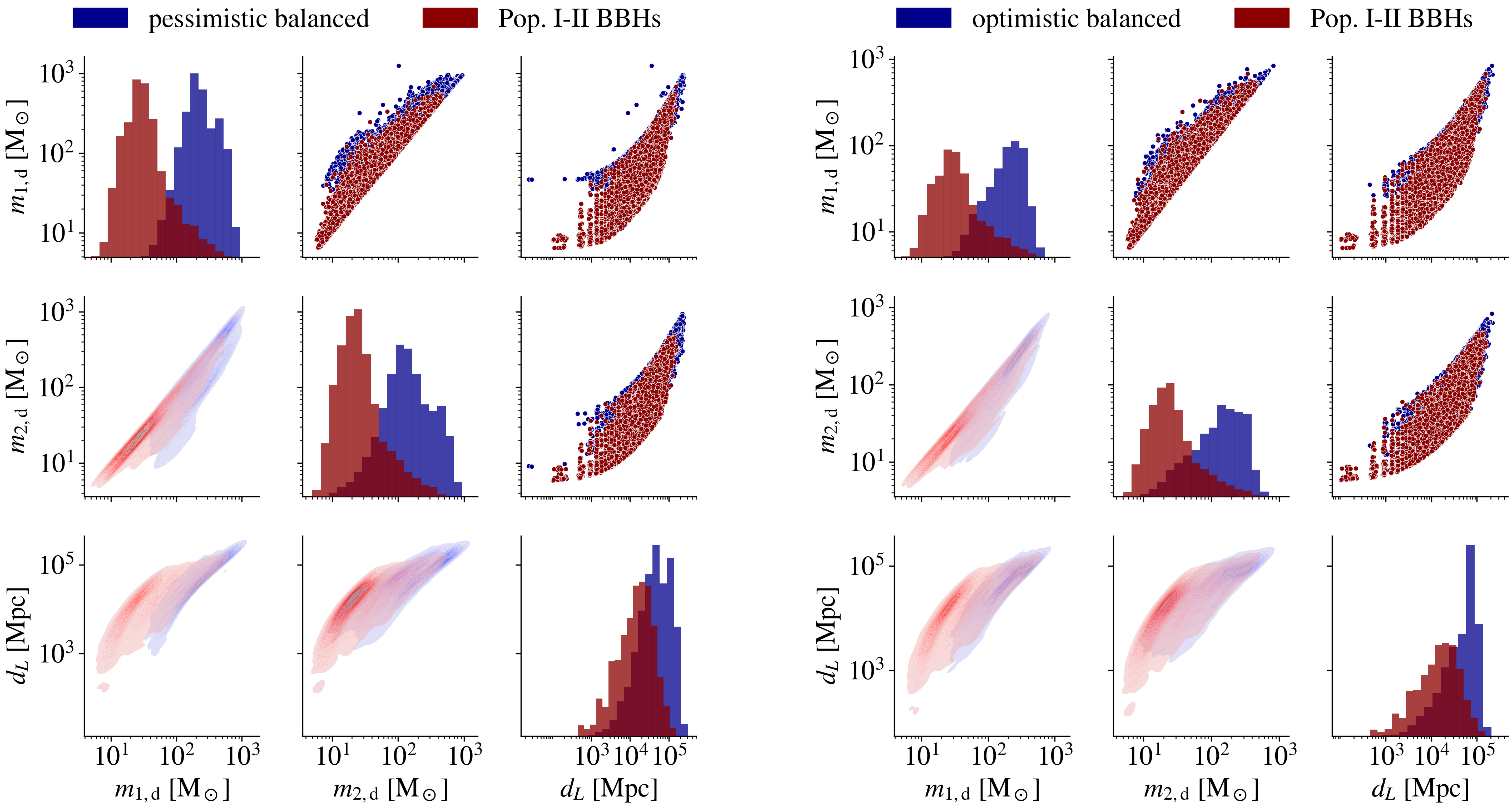

pessimistic balanced
Pop. I-II BBHs
optimistic balanced
Pop. I-II BBHs
$m_{1,\mathrm{d}}$ [$\mathrm{M}_\odot$]
$m_{2,\mathrm{d}}$ [$\mathrm{M}_\odot$]
d_L [Mpc]
10^1
10^2
10^3
10^5
10^4

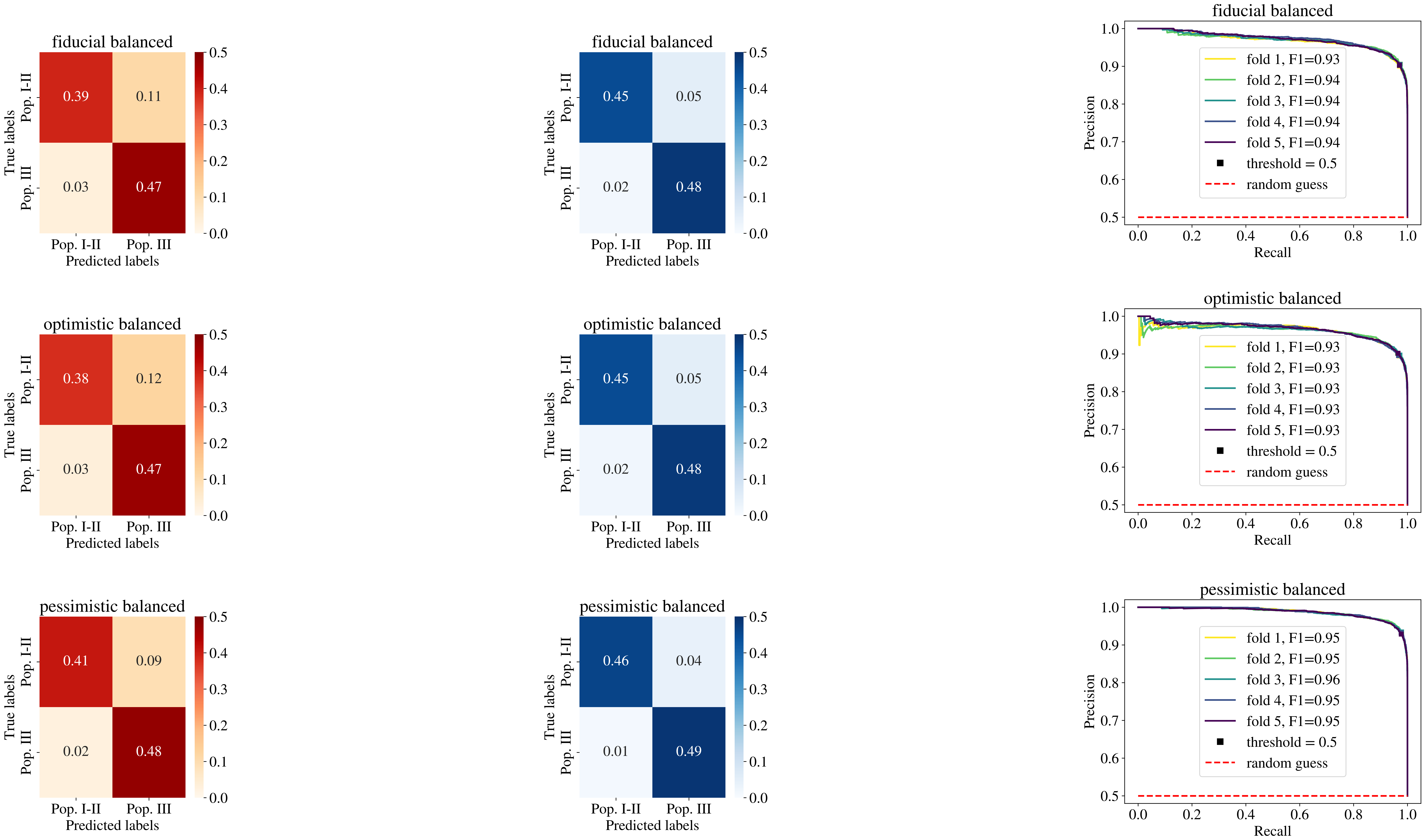
fiducial balanced
True labels
Pop. I-II
Pop. III
Predicted labels
0.39
0.11
0.03
0.47
0.45
0.05
0.02
0.48
optimistic balanced
0.38
0.12
0.03
0.47
0.45
0.05
0.02
0.48
pessimistic balanced
0.41
0.09
0.02
0.48
0.46
0.04
0.01
0.49
0.0
0.1
0.2
0.3
0.4
0.5
Precision
Recall
fold 1, F1=0.93
fold 2, F1=0.94
fold 3, F1=0.94
fold 4, F1=0.94
fold 5, F1=0.94
threshold = 0.5
random guess
fold 1, F1=0.93
fold 2, F1=0.93
fold 3, F1=0.93
fold 4, F1=0.93
fold 5, F1=0.93
fold 1, F1=0.95
fold 2, F1=0.95
fold 3, F1=0.96
fold 4, F1=0.95
fold 5, F1=0.95
0.6
0.7
0.8
0.9
1.0

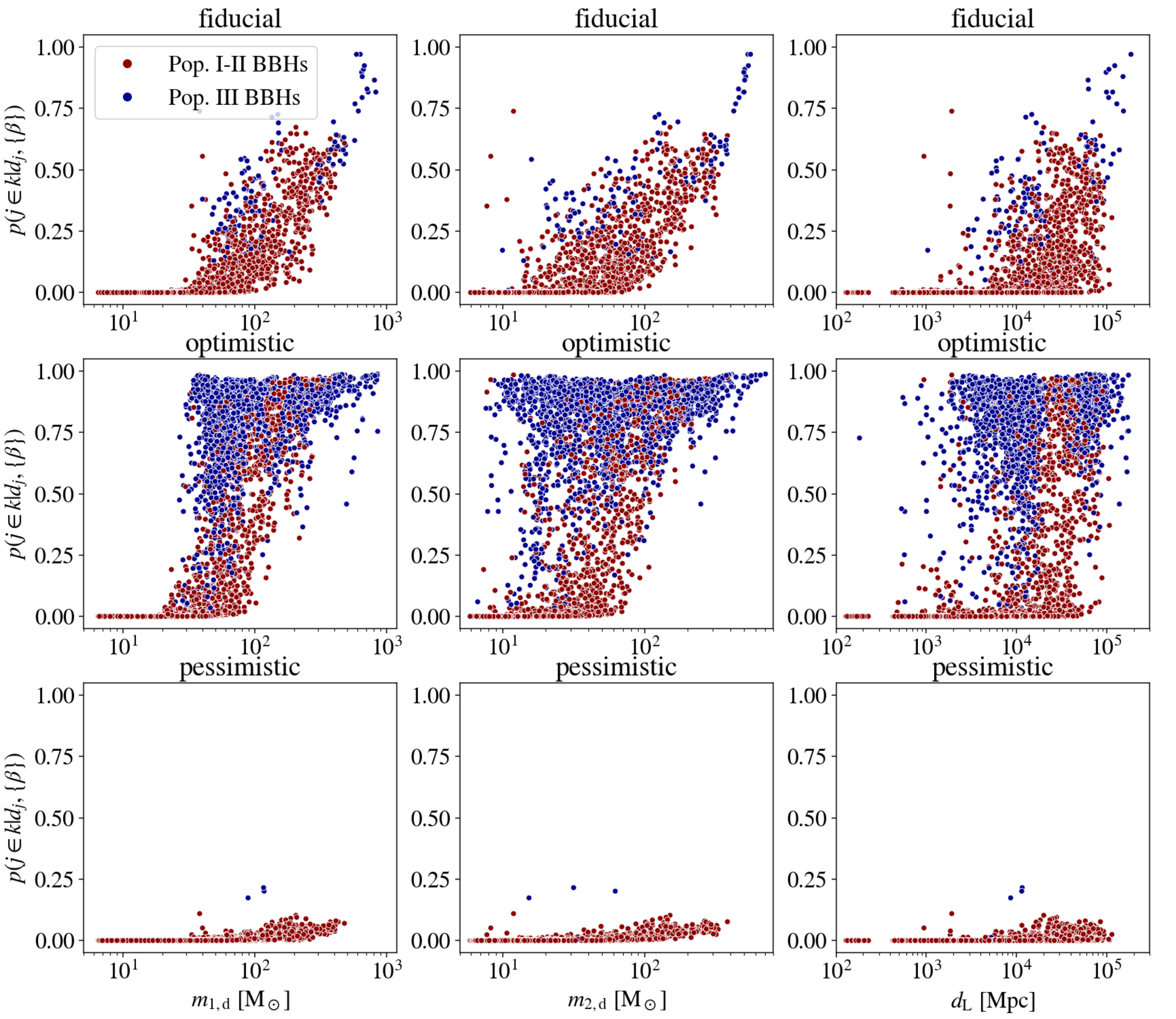

Fiducial

Thr.	%TP	%TN	%FP	%FN	Precision	Recall
0.1	96	85	15	4	0.20	0.96
0.2	86	90	10	14	0.26	0.86
0.5	33	98	2	67	0.43	0.33
0.7	11	100	0	89	0.94	0.11
0.9	3	100	0	97	1.00	0.03

Optimistic

Thr.	%TP	%TN	%FP	%FN	Precision	Recall
0.1	100	77	23	0	0.80	1.00
0.2	99	80	20	1	0.81	0.99
0.5	95	85	15	5	0.85	0.95
0.7	87	89	11	13	0.88	0.87
0.9	46	96	4	54	0.91	0.46

Pessimistic

Thr.	%TP	%TN	%FP	%FN	Precision	Recall
0.1	50	100	0	50	0.60	0.50
0.2	33	100	0	67	1.00	0.33
0.5	0	100	0	100	0	0
0.7	0	100	0	100	0	0
0.9	0	100	0	100	0	0